PERGAMON

Available online at www.sciencedirect.com
SCIENCE DIRECT®

Solid State Communications 128 (2003) 287–290

solid
state
communications

www.elsevier.com/locate/ssc

Preparation and characterization of oriented silica nanowires

S.H. Sun[a], G.W. Meng[a,b,*], M.G. Zhang[a,c], Y.T. Tian[a], T. Xie[a], L.D. Zhang[a]

[a]Institute of Solid State Physics, Chinese Academy of Sciences, P.O. Box 1129, Hefei 230031, People's Republic of China
[b]Department of Materials Science and Engineering, Rensselaer Polytechnic Institute, 1108th Street, Troy, NY 12180, USA
[c]Department of Materials Science and Engineering, Taiyuan Heavy Machinery Institute, Taiyuan 030024, People's Republic of China

Received 13 June 2003; accepted 26 August 2003 by T.T.M. Palstra

Abstract

Large-scale of oriented closely packed silica nanowire bunches have been synthesized by using large size (1–10 μm in diameter), low melting point tin droplets as catalyst on silicon wafers at 980 °C. Scanning electron microscopy (SEM) and transmission electron microscopy (TEM) analyses show that the amorphous silica nanowires have lengths of 50–100 μm and diameters of 100–200 nm. Unlike any previous observed results using high melting point metal (such as gold and iron) as catalyst, the Sn catalyst growth exhibits many interesting phenomena. Each Sn ball can simultaneously catalyze the growth of many silica nanowires, which is quite different from the conventional vapor–liquid–solid process.

PACS: 81.16.Hc; 68.65. − k

Keywords: A. Nanostructures; B. Nanofabrications; C. Scanning and transmission electron microscopy

1. Introduction

Researches on the synthesis of one-dimensional (1D) nanostructures have flourished in recent years because of their fundamental importance to nanotechnology [1]. Nanowires are particularly interesting as they offer the opportunity to investigate electrical and thermal transport process in size-confined systems, with the possibility of providing a deep understanding of physics at the nano-scale. Among them, silica nanowires have attracted considerable attention because of their unique properties and promising applications in mesoscopic research and optoelectronic nanodevices [2–5].

It is of interest to note that silicon oxide may form some novel morphology, such as silica 'nanoflowers' [6–8], radial pattern of carbonated silica fibers [9,10], silica nanowire 'bundles' and 'nanobrushes' arrays and silica nanotubes [11], tree-like and tadpole-like SiO_x nanostructures [12]. Most of the growth of the above-mentioned nanostructures could be explained by the vapor–liquid–solid (VLS) mechanism [13], which was proposed by Wagner and Ellis in 1964 for silicon whisker growth. Very recently, Liu et al. [14] have synthesized ultra-long and highly oriented silicon oxide nanowires via Ga as catalyst; Pan and his co-workers push the conventional VLS mechanism to a new range by using molten gallium as catalyst to grow highly aligned silica nanowires [15].

In this letter, we report a simple method to synthesize large quantities of closely packed silica nanowire bunches, by using tin (Sn) powders as catalyst and silicon wafers as a source material, via the extended VLS mechanism [15]. Further more, the possible growth mode corresponding to these novel structures was proposed in this paper.

2. Experimental

The synthesis of silica nanostructures was carried out in a high-temperature tube furnace. Briefly, an alumina tube was placed horizontally inside the tube furnace. An alumina boat loaded with pure Sn powders (99.9 wt%, 0.1 g) was

---

[*] Corresponding author. Tel.: +86-551-559-3060; fax: +86-551-559-1434.

E-mail address: qwmeng@issp.ac.cn (G.W. Meng).

0038-1098/$ - see front matter © 2003 Elsevier Ltd. All rights reserved.
doi:10.1016/j.ssc.2003.08.021

placed in the middle of the alumina tube, several pretreated Si wafers were placed one by one on a lone alumina plate, which was placed next to the alumina boat at the downstream end of the tube. The Si wafers were pretreated as follows. Several piece of strip-like Si (111) wafers were ultrasonically cleaned in ethanol, acetone in turn for 15 min, treated in piranha solution (30% H_2O_2/20% H_2SO_4), rinsed with de-ionized water and then dried in air.

Before heating, the tube was evacuated by a mechanical rotary pump to a base pressure of 5×10^{-2} Torr. And high-purity argon was poured in to clean away the impurity gas absorbed in the Si wafers, alumina boat and plate, and the tube wall. Then, the furnace was heated to 980 °C at a rate of 50 °C/min and held at this temperature for 2 h. During the experiment, high-purity (99.99%, $H_2O <$ or $= 20$ ppm, $O_2 <$ or $= 20$ ppm) argon was kept flowing through the tube at a rate of 100 sccm (standard cubic centimeters per minute), and the flow pressure in the alumina tube was kept at about 1 atm. The temperature between the tube center and the downstream end was measured in situ by a sheathed thermocouple, allowing us to readily measure the temperature in the silica nanowire formation region. After the furnace was cooled naturally to room temperature, white sponge-like products were found on the upper surface of the Si wafer located in the temperature range of 940–950 °C.

The as-synthesized products were characterized by scanning electron microscopy (SEM, JEOL JSM-6300), transmission electron microscopy (TEM, JEOL 2010). The chemical compositions were determined by X-ray photoemission spectra (XPS, VGESCALAB MKII) and energy-dispersive X-ray spectroscope (EDS) attached to SEM instrument. XPS data were collected in the constant analyzer energy (CAE) mode at 20 eV. Mg Kα($h\nu = 1253.6$ eV) radiation was employed as excitation source with an anode voltage of 12 kV and an emission current of 20 mA. For SEM observations, the product was pre-sputtered with a conducting layer of noble Pt metal, and then together with the Si wafer was directly transferred into SEM chamber. Specimens for TEM investigations were briefly ultrasonicated in ethanol, and then a drop of suspension was placed on a holey carbon copper grid.

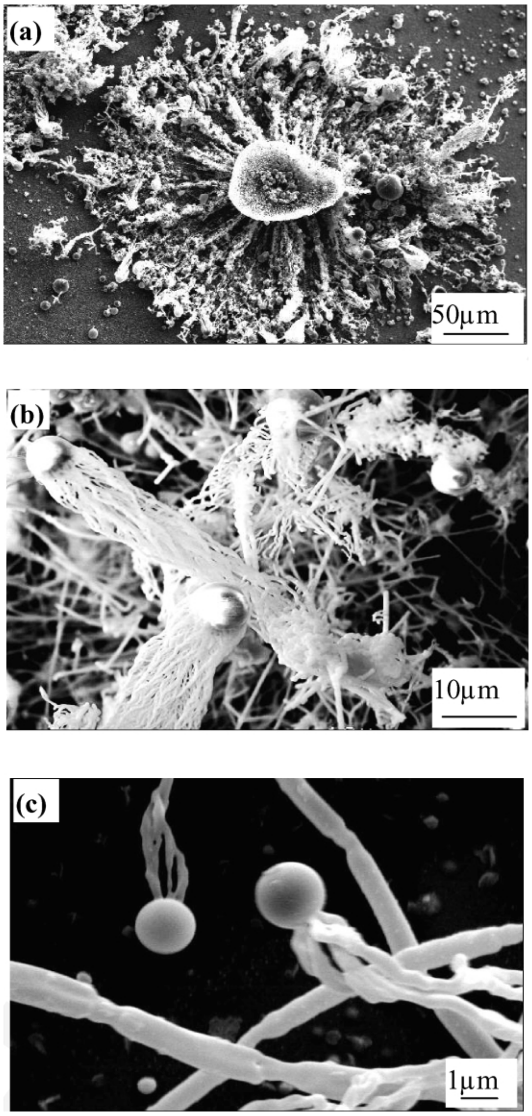

Fig. 1. SEM images of the as-synthesized products. (a) An overview of jellyfish-like microstructures. (b) Typical jellyfish-like microstructures with closely packed silica nanowires. (c) A SEM image of cherry-like structure.

3. Results and discussion

The morphology of the as-synthesized product was examined by SEM. A typical low-magnification SEM image (Fig. 1(a)) reveals the presence of large quantities of jellyfish-like microstructures with diameters of 2–10 μm and lengths of up to 50–100 μm, exhibiting a pronounced three dimensional feature. Each jellyfish-like structure terminates at its top end in a large spherical ball with a diameter comparable to that of the connected tail (Fig. 1(b)). The morphology of the jellyfish-like structures is similar to that of VLS-grown nanowires, suggesting that the growth of our products is likely governed by VLS mechanism. The tail part of the jellyfish-like structure is composed of large quantities of closely packed oriented nanowires with diameters of 100–200 nm and lengths of 50–100 μm. Quantitative EDS analyses of the jellyfish-like structure show that the nanowires have the composition of Si and O elements in atomic ratio of 1:2, closing to SiO_2; no other elements such as tin is detected; while the balls on the tops of the nanowires are composed of Sn, Si, and O. It is very interesting that each ball can simultaneously catalyze the growth of many SiO_2 nanowires, and the nanowires grow out perpendicularly from the low hemisphere surface of the ball, which is quite different from the conventional VLS mode in that one catalyst particle usually directs the growth of one nanowire. Detailed study reveals that split growth occurred in the silica nanowires, i.e. one nanowire splits into two or more (usually not more than five) sub-branches, and the newly formed branches sometimes also split into subbranches. The branches and the subbranches have similar growth direction and similar diameters to their stems, which is the same as the splitting phenomenon observed by Pan et al. in their gallium-catalyzed silica nanowires [15]. In some extra case, only several SiO_2 nanowires grow out from the ball, forming a cherry-like morphology shown in Fig. 1(c), and the ball is relatively smaller than that directing the growth of many SiO_2 nanowires.

Empirical SEM observations suggest that the number of the nanowires and the diameters of the balls connected with the nanowires are intimately related. For instance, from a comparison of the morphologies shown in the cross-section SEM image of the as-synthesized product (Fig. 2), it appears that the bigger the diameter of the ball, the more the SiO_2 nanowires grow out from the ball.

The morphology and structure of the nanowires have been characterized in further detail using TEM. The nanowires (Fig. 3(a)) have smooth surfaces with diameters of about 100–200 nm. Highly dispersed selected area electron diffraction pattern (inset in Fig. 3(a)) taken from many nanowires shows that the SiO_2 nanowires are amorphous, and the split growth of SiO_2 nanowires occurs (Fig. 3(b)), in agreement with SEM observations.

Further evidence for the formation of silica nanowires can be obtained through XPS. The two strong peaks at 531.6 and 102.6 eV as shown in Fig. 4(a) and (b) correspond to the binding energy of O (1s) and Si (2p) for silica, respectively.

On the basis of the conventional VLS growth mechanism and the experimental results described above, we have proposed a possible mechanism for the growth of the jellyfish-like silica nanowires. During the early period of heating, the hot Sn vapor generated from Sn powders rapidly condenses into small clusters as the Sn species become cool due to the collision with the buffer gas (argon, oxygen that remained in the reaction chamber). The formed Sn clusters are transferred to the downstream end of the alumina tube by the carrier gas and then deposit onto the surface of silicon wafers to grow into small liquid Sn droplets. The diameters of Sn droplets increase with the reaction time through continuously accepting the upcoming Sn clusters. The Si wafer was first dissolved in molten Sn at elevated temperature, i.e. the hot liquid Sn droplets etch the silicon wafer to form liquid Sn–Si alloy droplets. The solubility of Si in Sn at 950 °C is ~4 at.% [16]. The Si in the Sn–Si alloy evaporates into gas species to create a dense vapor of silicon species around the silicon wafer region, which is similar to that happened in Ga-catalyst growth of aligned silica nanowires [15]. In the meanwhile, the liquid alloy droplet could also absorb Si from the vapor. Then, the dissolved silicon was oxidized by the oxygen (the source of oxygen will be discussed latter). Since silicon oxide is not soluble in tin, it had to precipitate out of the alloy droplet in a form of silicon oxide nanoparticles [15]. The growth of silica nanowires can be broken down to four steps:

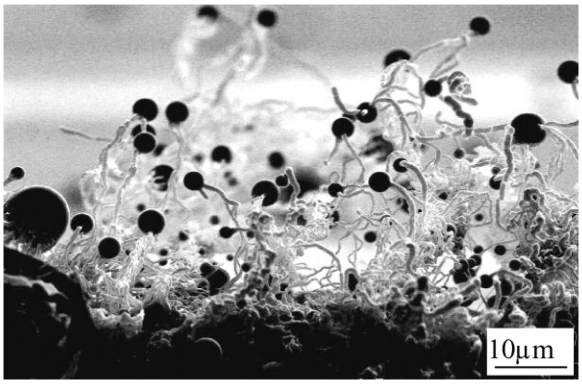

Fig. 2. Cross-section SEM image of the as-synthesized product.

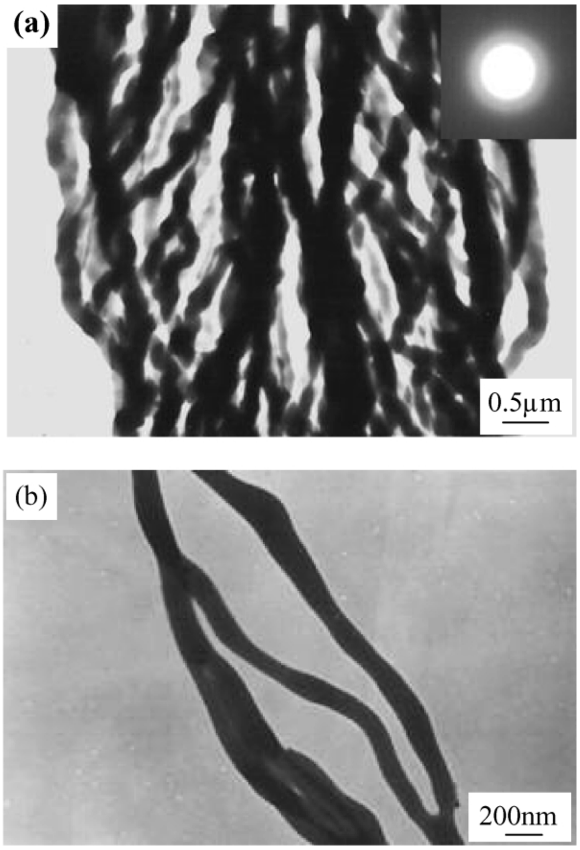

Fig. 3. TEM images of the as-synthesized products. (a) The fine morphology of the tail part of the jellyfish-like structure, the highly dispersed SAED ring pattern (inset) showing that the nanowires are amorphous. (b) A more detailed TEM image showing the splitting growth in SiO_2 nanowires.

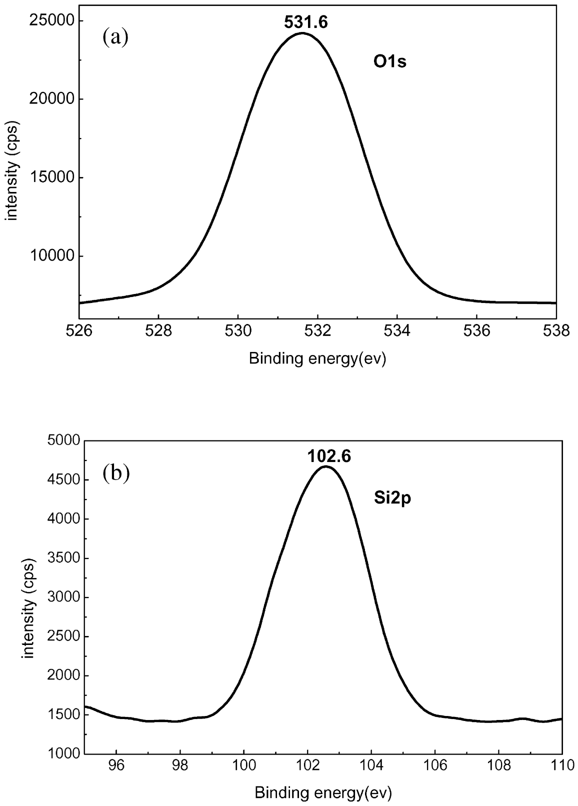

Fig. 4. XPS spectra of the silica sample. (a) O1s binding energy spectrum; (b) Si2p binding energy spectrum.

- The formation of silicon oxide nanoparticles on the Sn–Si alloy surface due to the low solubility of silicon oxide in Sn.
- These nanoparticles act as the nucleation sites, initiating the growth of silica nanowires.
- The alloy droplets continuously absorbing Si species from the vapor.
- These nanowires may subsequently grow toward each other, and then coalesce into one, forming the branched nanostructures in the end [7].

The source of oxygen that contributed to the formation of silica nanowires may have several origins. The most likely source of oxygen may come from the low content of H_2O (~ 20 ppm) and O_2 (~ 20 ppm) in the carrier gas of Ar, which can supply a constant oxygen source during the growth process of silica nanowires. The residual oxygen may also be a source, as the base pressure (5×10^{-2} Torr) of the vacuum system was relatively high. The leakage of reaction system can be ignored under the pressure of 1 atm.

More work is underway to better understand the growth mechanism and to prepare nanowires with different diameters and/or different materials.

4. Conclusions

Closely packed SiO_2 nanowire bunches have been produced in high yield on Si wafer using Sn as catalyst. The Sn-catalyst growth shows many interesting new phenomena, which are different from any previously achieved results using Au, Fe, and Ni as catalysts. The use of Sn as catalyst provides a new way for nanowire growth and extends the conventional VLS mechanism to a broader range. In addition, the method reported here may be exploited to produce nanowires of other materials by using Sn as catalyst.

Acknowledgements

We thank Professor Yongqiang Mao and Yong Qin for their technical assistance. This work was supported by the Ministry of Science and Technology of China (Grant No. G1999064501) and the National Natural Science Foundation of China (Grant No. 19974055 and 50271068).

References

[1] B.I. Yakobson, R.E. Smalley, Am. Sci. 85 (1997) 324.
[2] S. Manm, G.A. Ozin, Nature 382 (1996) 313.
[3] W. Wesh, N.I. Meth, Phys. Rev. B 116 (1996) 305.
[4] A. Katz, M.E. Davis, Nature 403 (2000) 286.
[5] C.T. Kresge, M.W. Leonowiez, W.J. Roth, J.C. Vartvli, J.S. Boch, Nature 359 (1999) 710.
[6] Y.Q. Zhu, W.B. Hu, W.K. Hsu, M. Terrones, N. Grobert, T. Karali, H. Terrones, J.P. Hare, P.D. Townsend, H.W. Kroto, D.R. Mwalton, Adv. Mater. 11 (1999) 844.
[7] Y.Q. Zhu, W.K. Hsu, M. Terrones, N. Grobert, W.B. Hu, J.P. Hare, H.W. Kroto, D.R.M. Walton, Chem. Mater. 11 (1999) 2709.
[8] Y.Q. Zhu, W.H. Hsu, M. Terrones, N. Grobert, H. Terrones, J.P. Hare, H.W. Kroto, D.R.M. Walton, J. Mater. Chem. 8 (1998) 1859.
[9] Z.J. Zhang, G. Ramanath, P.M. Ajiayan, D. Goldberg, Y. Bande, Adv. Mater. 13 (2001) 197.
[10] Z.J. Zhang, P.M. Ajiayan, G. Ramanath, Appl. Phys. Lett. 78 (2001) 3794.
[11] Z.L. Wang, R.P. Gao, J.L. Gole, J.D. Stout, Adv. Mater. 12 (2000) 1938.
[12] Y.J. Chen, J.B. Li, J.H. Dai, Chem. Phys. Lett. 344 (2001) 450.
[13] R.S. Wagner, W.C. Ellis, Appl. Phys. Lett. 4 (1964) 89.
[14] B. Zheng, Y.Y. Wu, P.D. Yang, J. Liu, Adv. Mater. 14 (2002) 122.
[15] Z.W. Pan, Z.R. Dai, C. Ma, Z.L. Wang, J. Am. Chem. Soc. 124 (2002) 1817.
[16] T.B. Massalski, H. Okamoto, P.R. Subramanian, L. Kacprozak, Binary Alloy Phase Diagrams, 2nd ed., ASM Int, Materials Park, OH, 1992.